Measurements of the Thermal Conductivity of HFC-134a in the Supercritical Region[†]

B. Le Neindre,*[,‡] Y. Garrabos,[§] F. Gumerov,[||] and A. Sabirzianov[||]

L.I.M.H.P.-C.N.R.S., Institut Galilée, Université Paris Nord, 99 Av. J. B. Clément, 93430 Villetaneuse, France, and ICMCB-CNRS UPR 9048, Université Bordeaux I, 87 Av du Dr A. Schweitzer, F 33608 PESSAC Cedex, France, and Kazan State Technological University, 68 K. Marx Street, Kazan, 420015 Tatarstan, Russia

Measurements of the thermal conductivity of HFC-134a made in a coaxial cylinder cell operating in steady state are reported. Measurements were performed along several quasi-isotherms at temperatures ranging from the critical temperature T_c (~374 K) to T_c + 150 K and in a pressure range from (0.1 to 40) MPa. Parameters of a background equation were determined from experimental data to analyze the critical enhancement of the thermal conductivity as a function of temperature and density. An analysis of the various sources of errors leads to an estimated uncertainty of the thermal conductivity data of ± 3 %.

Introduction

In the past years, there has been a great industrial interest in the determination of the thermophysical properties of alternative refrigerants. In our laboratory, we have carried out a series of measurements of the thermal conductivity of several alternative refrigerants over a large range of temperature (T) and pressure (p), including the subcritical and supercritical regions.[1,2] Among them, HFC-134a (1,1,1,2-tetrafluoroethane) was considered for a long time as an environmentally acceptable alternative refrigerant to CFC-12 (dichlorodifluoromethane). Some previous measurements[3] of the thermal conductivity of HFC-134a have been already performed, along several quasi-isotherms between (300 and 530) K and from (0.1 to 50) MPa. The present thermal conductivity measurements of HFC-134a were carried out as a function of temperature between T_c (~374 K) and T_c + 150 K and pressures up to 40 MPa, including then the homogeneous critical region, using vertical coaxial cylinders, operating in the steady state mode. This method of measurement and the applied corrections were previously described.[4] During the experiments, the stability of the temperature was kept better than 0.05 K, and the precision of temperature measurements was ± 0.05 K. The pressure was measured with a precision pressure transducer with accuracy of 0.02 %. The consistency of pressure and temperature measurements was checked along the saturation pressure curve with vapor pressures calculated from the equation of state developed by Tillner-Roth and Baehr.[5] The purity of the sample was estimated to be better than 99.9 % by the manufacturer's analysis and appears to conform with the purity specifications (especially for water contamination) of the Round-Robin samples of R134a.[6] New experimental results are reported in Table 1 for the dilute gas state (near 1 bar pressure) and in Table 3 to Table 17 for the fluid dense state along 15 quasi-isotherms, up to 21 MPa. The nominal temperature is the temperature at the critical density. The density (ρ) was calculated with the equation of state developed by Tillner-Roth and Baehr,[5] with accuracy of the order of ± 0.2 % in the critical region as stated by the authors. In fact, the accuracy can be much lower, close to the critical point, and can reach ± 2 %. The critical parameters together with the estimated uncertainties are given as follows

Table 1. Thermal Conductivity of HFC-134a Near Atmospheric Pressure

T / K	p / MPa	λ_0(exp) / mW·m^{-1}·K^{-1}	100·[(λ_0(cal) − λ_0(exp)]/λ_0(exp) [λ_0(cal) from eq 5]
299.29	0.17	12.87	–0.27
299.63	0.17	12.79	0.59
318.97	0.74	14.89	–1.64
318.97	0.74	14.86	–1.44
319.14	0.16	14.60	0.42
345.58	0.18	17.11	–0.09
346.36	0.18	17.39	–1.28
348.54	0.18	17.32	0.27
351.84	0.64	17.63	0.23
363.88	0.18	18.91	–0.69
365.00	0.18	18.91	–0.15
365.41	0.18	18.93	–0.05
365.69	0.18	18.93	0.08
366.52	0.18	18.92	0.54
366.80	0.18	18.93	0.62
372.42	0.68	19.75	–0.94
372.43	0.17	19.68	–0.58
372.43	0.68	19.65	–0.43
378.07	0.18	20.03	0.28
378.63	0.44	20.17	–0.16
378.74	0.18	20.12	0.13
378.90	0.33	20.26	–0.49
379.17	0.30	20.23	–0.21
379.43	0.15	20.35	–0.69
379.72	0.16	19.96	1.39
392.65	0.18	21.36	0.31
426.86	0.16	24.69	–0.46
436.44	0.18	25.42	0.15
446.25	0.20	26.65	–1.09
446.25	0.76	26.61	–0.94
451.17	0.18	26.83	–0.06
455.69	0.10	26.80	1.60
455.92	0.68	27.19	0.22
466.31	0.65	28.46	–0.89
476.24	0.10	29.22	–0.34
496.18	0.10	31.10	–0.46
515.97	0.10	33.04	–0.80

* Corresponding author. E-mail: leneindr@limhp.univ-paris13.fr.
[†] Part of the "William A. Wakeham Festschrift".
[‡] Université Paris Nord.
[§] Université Bordeaux I.
[||] Kazan State Technological University.

10.1021/je900210h CCC: $40.75
Published on Web 06/12/2009

$T_c = (374.21 \pm 0.06)$ K, $p_c = (4.05928 \pm 0.016)$ MPa, and $\rho_c = (511.9 \pm 4)$ kg·m^{-3} (1)

The measurements were carried out to make an analysis of the data based on the residual method. The thermal conductivity data are covering the supercritical region ($T > T_C$) of the p, ρ, T phase surface, corresponding to three main parts, i.e., the gaseous state ($\rho \sim 0$) at $p = 1.01325$ bar, the moderate ($0 < \rho \leq 1.2\rho_c$), and the high ($\rho > 1.2\rho_c$) dense states, respectively. Consequently, the thermal conductivity expressed as a function of temperature and density was separated into three parts

$$\lambda(T,\rho) = \lambda_0(T) + \delta\lambda(\rho) + \Delta\lambda_c(T,\rho) \quad (2)$$

where $\lambda_0(T)$ is the dilute gas thermal conductivity which is only a function of temperature at $\rho = 0$, $\delta\lambda(\rho)$ is the residual thermal conductivity which is only a function of density, and $\Delta\lambda_c(T,\rho)$ is the critical enhancement approaching the liquid−gas critical point. In that description, the two first contributions of eq 2 represent the background thermal conductivity

$$\lambda_b(T,\rho) = \lambda_0(T) + \delta\lambda(\rho) \quad (3)$$

To determine $\lambda_b(T,\rho)$, we have considered the data in the high dense phase and in the gas phase at atmospheric pressure and far from the critical temperature ($T > 385$ K) region, including then the related parts of our previous measurements reported in ref 3. The resulting critical enhancement $\Delta\lambda_c(T,\rho)$ of the thermal conductivity is given in column 5 of Tables 3 to 17. The uncertainties of the thermal conductivity measurements were estimated to be of the order of ± 3 %. The main error is due to the measurement of the temperature difference between the concentric cylinders.

We note that several other measurements of the thermal conductivity of R134a were performed under pressure, for instance those of Assael et al.,[7] with an estimated accuracy of 0.5 %. At supercritical temperatures from (390 to 450) K and at pressures to 70 MPa, Perkins et al. have reported several sets of data obtained with a transient hot-wire cell.[8,9]

Dilute-Gas Thermal Conductivity

The thermal conductivity data measured at atmospheric pressure in the temperature range (299 to 516) K are presented in Table 1. As a theoretical calculation of the thermal conductivity of a polar fluid in the dilute-gas region requires several parameters which are difficult to evaluate with a good accuracy,[3] these experimental data were fit to an empirical linear equation

$$\lambda_0 = a_0 + a_1 T \quad (4)$$

where λ_0 and T are expressed in mW·m^{-1}·K^{-1} and K, respectively. Fitting the complete set of the 37 data of Table 1 and the 32 data given in ref 3, the related values of two adjustable parameters are $a_0 = -14.7107$ mW·m^{-1}·K^{-1} and $a_1 = 0.0920389$ mW·m^{-1}·K^{-2}. The relative deviation between the experimental data and the theoretical values calculated using eq 4 are reported in Table 1 and shown in Figure 1 for the complete data set. The related 1σ-standard deviation of 0.70 % is also illustrated in Figure 1, which appears within our estimated experimental uncertainty of 1.5 % (i.e., approximately 2σ, see ref 3) in this range of measurement.

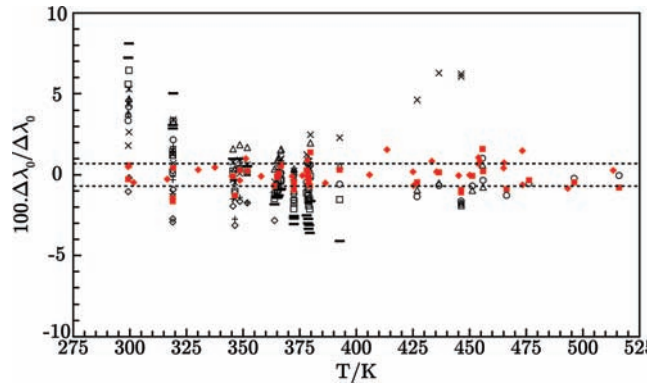

Figure 1. Fractional deviation $100 \cdot \Delta\lambda_0/\lambda_0 = 100 \cdot [\lambda_0(\text{cal}) - \lambda_0(\text{exp})]/\lambda_0(\text{exp})$ of the dilute gas thermal conductivity of R134a as a function of temperature. This work: ■ (Table 1) and ◆ Le Neindre and Garrabos (ref 3), where the calculated values were obtained from eq 4. From experimental values of Table 1 and calculated values obtained from the analytical correlations reported in Table 2: ×, Perkins et al.;[8,9] *, Soldner et al.;[10] −, Krauss et al.;;[11] △, Hammerschmidt;[12] □, Tsvetkov et al.;[13] +, Gross et al.;[14] ◇, Tanaka et al.;[15] ○, Yata et al.[16] The dashed lines are one standard deviation of the fit of our complete experimental data set using eq 4 (see text).

In Table 2 are listed similar analytic equations (up to the third order) that have been reported in the literature[8–16] to

Table 2. Representative Equations of the Thermal Conductivity λ_0 of R134a, at Atmospheric Pressure

equation	coefficients	T-range/K	sd (σ) (%)	ref
$\lambda_0 = a_0 + a_1 T$	$a_0 = -14.7107$ $a_1 = 0.0920389$	299 to 516	0.70 (69 data)	this work
$\lambda_0 = a_0 + a_1 T + a_2 T^2$	$a_0 = 5.79393$ $a_1 = -0.0283907$ $a_2 = 0.176461 \cdot 10^{-3}$	200 to 450	2.43 (52 data)	8, 9
$\lambda_0 = a_0 + a_1 T + a_2 T^2$	$a_0 = -17.314$ $a_1 = 0.12048$ $a_2 = -0.5926 \cdot 10^{-4}$	294 to 363	1.89 (19 data)	10
$\lambda_0 = a_0 + a_1 T + a_2 T^2$	$a_0 = -16.5744$ $a_1 = 0.124286$ $a_2 = -0.761796 \cdot 10^{-4}$	240 to 410	3.12 (41 data)	11
$\lambda_0 = a_0 + a_1 T$	$a_0 = -12.68$ $a_1 = 0.087$	298 to 463	1.43 (58 data)	12
$\lambda_0 = a_0 + a_1 T + a_2 T^2 + a_3 T^3$	$a_0 = -1.203289$ $a_1 = 0.020169658$ $a_2 = 0.113395 \cdot 10^{-4}$ $a_3 = -0.5232105 \cdot 10^{-7}$	240 to 400	2.33 (40 data)	13
$\lambda_0 = a_0 + a_1 t^a$	$a_0 = 11.3853$ $a_1 = 0.0754957$	250 to 360	2.42 (18 data)	14
$\lambda_0 = a_0 + a_1 T$	$a_0 = -13.39$ $a_1 = 0.0872932$	293 to 363	0.85 (19 data)	15
$\lambda_0 = a_0 + a_1 (T/T_c) + a_2 (T/T_c)^{2b}$	$a_0 = -6.3643$ $a_1 = 19.099$ $a_2 = 6.8704$	200 to 600	1.25 (69 data)	16

[a] $t = T - 273.15$ K. [b] $T_c = 374.27$ K.

Table 3. Thermal Conductivity of HFC-134a along the Quasi-Isotherm 374.37 K

T / K	p / MPa	ρ / kg·m^{-3}	λ / mW·m^{-1}·K^{-1}	$\Delta\lambda_c$ / mW·m^{-1}·K^{-1}
379.43	0.154	5.0	23.1	0.1
375.04	0.888	31.6	23.5	0.2
376.38	2.200	91.9	25.2	0.2
376.23	2.350	100.6	25.6	0.3
375.93	2.700	123.4	26.5	0.6
375.76	3.000	146.4	27.4	0.8
375.59	3.196	164.1	28.7	1.5
375.42	3.349	180.1	29.8	2.2
375.10	3.544	205.0	32.1	3.7
374.92	3.675	225.8	34.2	5.1
374.76	3.717	234.2	35.2	5.8
375.34	3.828	252.4	36.7	6.6
375.14	3.928	280.5	40.9	9.9
375.10	3.981	299.7	42.8	11.1
375.18	4.030	320.4	47.9	15.3
374.89	4.035	332.3	49.4	16.3
374.72	4.049	350.4	52.9	19.1
374.66	4.063	369.7	59.3	24.4
374.61	4.068	382.1	67.4	31.7
374.57	4.073	397.9	76.4	39.8
374.54	4.072	400.5	83.1	46.1
375.24	4.120	403.9	101.6	63.6
374.47	4.071	408.6	109.6	71.1
374.39	4.070	436.4	164.4	122.7
374.37	4.073	529.9	197.4	150.6
374.37	4.074	554.1	197.4	149.5
374.38	4.078	584.3	182.8	133.9
374.38	4.083	605.8	174.2	124.5
374.28	4.085	632.7	141.0	91.1
374.31	4.090	635.3	123.3	74.1
374.32	4.093	637.9	113.9	64.9
374.34	4.097	640.2	105.7	57.0
374.36	4.100	641.2	99.3	50.8
374.38	4.105	644.4	91.4	43.0
374.40	4.110	647.4	85.1	36.8
374.18	4.090	652.3	72.9	25.0
374.19	4.100	660.1	70.8	22.6
374.21	4.120	672.4	68.0	19.2
374.22	4.142	683.7	65.9	16.6
374.22	4.149	686.9	65.4	15.8
374.23	4.187	701.3	64.2	13.9
374.37	4.245	713.2	64.3	13.3
374.37	4.270	719.6	64.3	12.9
374.37	4.358	737.9	64.1	11.6
374.50	4.533	761.2	63.7	9.7
374.51	4.621	771.3	63.5	8.8
374.52	4.710	780.4	61.7	6.5
374.52	4.759	785.0	61.0	5.5

represent the temperature variation of the thermal conductivity of R134a at atmospheric pressure. The values of their adjustable coefficients are reported in column 2, while their respective temperature range of validity is given in column 3, covering then the complete temperature range from (200 to 600) K. The corresponding 1σ-standard deviation from our experimental results given in Table 1 is reported in column 4, which clearly shows the weakness of some analytic equations.[8,9,11,13] These systematic deviations of the temperature dependence of the thermal conductivity of the dilute gas are also illustrated in Figure 1, while this figure simultaneously reveals the noticeable agreement between the experimental data obtained by static methods.[12,15] As was mentioned in ref 17, the uncertainty at low densities is much larger than that at higher densities due to the large inner and outer boundary corrections in transient hot-wire measurements. Therefore, Figure 1 indicates that the experimental data generally agree with the linear correlation of eq 4 within an uncertainty of 2σ, especially for the temperature range (300 to 600) K. Such a linear form can be of practical interest to complement our previous theoretical dilute gas

Table 4. Thermal Conductivity of HFC-134a along the Quasi-Isotherm 374.96 K

T / K	p / MPa	ρ / kg·m^{-3}	λ / mW·m^{-1}·K^{-1}	$\Delta\lambda_c$ / mW·m^{-1}·K^{-1}
376.96	2.027	82.2	21.8	−0.2
376.51	2.527	111.3	22.9	0.2
376.33	3.030	148.0	24.2	0.5
375.81	3.534	201.0	27.9	2.8
375.46	4.029	312.9	39.7	11.2
375.43	4.051	324.8	42.5	13.7
375.34	4.085	350.9	51.7	22.0
375.30	4.089	356.4	57.3	27.5
375.11	4.099	381.3	67.1	36.4
375.07	4.097	382.1	77.3	46.6
375.03	4.099	389.6	91.0	60.0
374.99	4.107	413.7	110.6	78.7
374.97	4.112	437.0	117.6	84.9
374.96	4.117	470.7	123.2	89.2
374.96	4.119	486.3	124.4	89.7
374.96	4.126	543.3	124.4	87.2
374.97	4.132	571.9	119.8	81.2
375.00	4.149	611.8	101.0	60.4
375.03	4.155	616.9	91.0	50.2
375.04	4.160	623.0	86.1	44.9
375.06	4.168	630.7	79.6	38.1
375.10	4.185	643.8	70.4	28.1
375.13	4.199	652.6	64.3	21.6
375.14	4.216	663.2	61.2	17.8
375.16	4.244	676.8	58.6	14.5
375.17	4.289	694.1	56.5	11.4
375.18	4.340	709.0	55.0	9.0
375.19	4.379	711.3	54.6	8.4
375.20	4.456	733.5	53.0	5.4
375.19	4.458	734.1	54.1	6.5
375.19	4.551	748.9	54.5	6.0
375.19	4.557	749.8	53.8	5.3
375.18	5.054	799.6	55.7	3.9
375.18	5.057	799.6	55.0	3.1
375.03	6.045	854.6	57.6	1.8
375.01	8.053	915.5	61.5	1.1
374.99	10.033	954.6	64.0	0.4

function that represents λ_0 (see eqs 4 to 6 of ref 3). In spite of the difficulty to calculate accurately the contributions from internal degrees of freedom, this theoretical estimation gives a 1σ-standard deviation of 0.94 % from our λ_0(exp) data set. However, we note that the correct C_P° temperature exponent of the right-hand side of eq 6 given in ref 3 is i, and not $i - 1$.

Dense Fluid Thermal Conductivity

To determine the residual density term $\delta\lambda(\rho)$ of the thermal conductivity, we have used our present measurements in the high dense phase and in the gas phase outside the critical region, in a temperature range from (300 to 550) K and pressure up to 50 MPa, including some related data already reported in ref 3. This density-dependent term of the thermal conductivity was then represented by the following six-order polynomial dimensionless form

$$\frac{\delta\lambda(\rho)}{\Lambda_C} = \sum_{i-1}^{6} l_i \left(\frac{\rho}{\rho_c}\right)^i \tag{5}$$

where Λ_C is the reference value of the critical thermal conductivity defined as

$$\Lambda_C = \frac{R^{5/6} P_c^{2/3}}{T_c^{1/6} M^{1/2} N_A^{1/3}} = 2.053 \text{ mW·m}^{-1}\text{·K}^{-1} \tag{6}$$

By fitting experimental data with eq 5, we have obtained the following values of the adjustable parameters

$l_1 = 6.02829$, $l_2 = 2.36295$, $l_3 = -4.43933$, $l_4 = 6.20601$, $l_5 = -2.80918$, and $l_6 = 0.451252$

with $\rho_c = 511.9$ kg·m^{-3}. The 1σ-standard deviations between calculated and experimental thermal conductivity values are within the uncertainty of the measurements, which was estimated to ± 1.5 %. We note that similar dimensionless correlations of eq 5 with different magnitude of σ were reported by Krauss et al.[11] and Yata et al.[16]

Critical Enhancement

The following analysis of the thermal conductivity and diffusivity of R134a in the critical region was carried out in terms of the effective values of the critical exponents, using a similar approach of the crossover modeling initially proposed by Luettmer-Strathmann and Sengers[18] to describe the singular behavior of the thermal diffusivity $D_T = \lambda/(\rho C_p)$. C_p is the isobaric specific heat capacity. As noted previously, the value of the critical enhancement term $\Delta\lambda_c(T, \rho)$ of the thermal conductivity was estimated by subtracting the background thermal conductivity term $\lambda_b(T, \rho)$ of eq 3 from the experimental data. The above separation of the thermal conductivity into critical and background contributions implies a corresponding separation of the thermal diffusivity D_T into a critical contribution $\Delta D_c = (\Delta\lambda_c)/(\rho C_p)$ and a background contribution $D_b = \lambda_b/(\rho C_p)$, with

$$D_T = \Delta D_c + D_b \tag{7}$$

The mode coupling of critical dynamics theory[19] predicts that ΔD_c of a critical pure fluid in the hydrodynamic limit can be written asymptotically near its critical point as

$$\Delta D_c = R_D \frac{k_B T}{6\pi\eta\xi} \tag{8}$$

where η is the shear viscosity; and ξ is the long-range correlation length of the density fluctuations. The prefactor R_D is a universal amplitude combination whose value is close to unity.[19] Along

Table 5. Thermal Conductivity of HFC-134a along the Quasi-Isotherm 375.14 K

T/K	p/MPa	ρ/kg·m^{-3}	λ/mW·m^{-1}·K^{-1}	$\Delta\lambda_c$/mW·m^{-1}·K^{-1}
376.23	3.734	228.5	30.1	4.1
376.21	3.800	240.3	31.2	4.9
376.01	3.908	265.0	34.0	7.0
375.99	3.936	272.4	34.9	7.7
375.95	3.993	289.9	37.4	9.6
375.65	4.023	306.1	39.3	11.0
375.61	4.059	324.0	42.5	13.7
375.60	4.065	327.6	43.2	14.3
375.53	4.097	351.8	49.2	19.5
375.51	4.107	361.8	52.1	22.0
375.46	4.118	377.4	59.1	28.6
375.40	4.126	395.1	68.3	37.1
375.37	4.128	402.6	76.3	44.9
375.33	4.129	410.6	87.0	55.2
375.32	4.130	414.8	91.6	59.7
375.15	4.130	460.7	105.5	71.9
375.14	4.132	477.2	107.2	72.9
375.14	4.134	490.4	108.0	73.1
375.14	4.136	504.2	108.0	72.6
375.14	4.138	517.8	108.0	72.0
375.14	4.140	530.9	108.0	71.4
375.14	4.142	543.0	107.2	70.0
375.14	4.144	553.8	106.3	68.7
375.15	4.146	559.1	104.7	66.8
375.15	4.148	567.9	102.4	64.0
375.16	4.150	572.1	100.9	62.3
375.16	4.153	582.6	98.8	59.7
375.17	4.157	591.3	94.1	54.6
375.18	4.160	596.4	91.6	51.9
375.19	4.163	600.9	88.1	48.1
375.20	4.166	605.0	84.9	44.6
375.21	4.170	610.6	82.3	41.8
375.21	4.171	612.3	81.4	40.8
375.23	4.178	619.9	77.7	36.7
375.23	4.181	624.1	76.0	34.7
375.24	4.189	632.4	73.1	31.4
375.28	4.208	646.2	66.7	24.3
375.30	4.229	659.6	62.7	19.5
375.31	4.254	672.8	61.3	17.4
375.31	4.265	677.9	61.0	16.8
375.31	4.294	689.6	60.5	15.6
375.31	4.307	694.1	60.3	15.1
375.31	4.341	704.5	60.0	14.2
375.32	4.389	716.4	59.2	12.7
375.32	4.450	729.1	58.5	11.2
375.32	4.490	736.3	58.8	11.0
375.46	4.735	766.6	58.2	8.5
375.48	4.848	777.8	56.6	6.1

Table 6. Thermal Conductivity of HFC-134a along the Quasi-Isotherm 375.28 K

T/K	p/MPa	ρ/kg·m^{-3}	λ/mW·m^{-1}·K^{-1}	$\Delta\lambda_c$/mW·m^{-1}·K^{-1}
376.07	0.200	6.6	20.5	0.5
376.06	0.524	17.9	20.8	0.5
376.05	0.773	27.1	21.2	0.7
376.04	1.048	37.8	21.4	0.6
375.95	2.429	105.6	23.5	1.0
375.94	2.662	120.7	24.0	1.1
375.90	2.970	143.7	25.1	1.5
375.87	3.165	160.6	26.1	2.1
375.87	3.264	170.1	26.4	2.1
375.80	3.504	197.2	29.0	4.0
375.76	3.658	218.7	30.6	4.9
375.73	3.772	238.2	31.9	5.7
375.69	3.874	259.9	34.3	7.5
375.66	3.917	271.0	36.1	8.9
375.63	3.965	285.4	37.8	10.2
375.61	3.999	297.4	39.5	11.6
375.58	4.040	315.2	42.1	13.6
375.56	4.055	323.3	43.4	14.6
375.52	4.086	343.8	47.5	18.1
375.49	4.097	353.8	50.8	21.0
375.46	4.107	364.8	54.5	24.4
375.42	4.115	376.7	61.1	30.5
375.36	4.121	390.9	72.1	41.1
375.34	4.126	402.6	77.3	45.9
375.32	4.134	426.0	85.6	53.3
375.29	4.139	452.9	94.3	61.0
375.28	4.145	488.8	98.6	63.8
375.28	4.150	518.5	100.2	64.1
375.28	4.156	550.4	100.2	62.6
375.28	4.162	574.4	99.4	60.7
375.28	4.167	589.2	98.4	58.9
375.29	4.174	602.8	95.5	55.4
375.30	4.181	613.4	92.7	52.1
375.31	4.189	623.4	88.9	47.7
375.32	4.197	631.6	84.8	43.2
375.33	4.204	637.7	81.6	39.7
375.36	4.216	645.4	74.6	32.2
375.38	4.225	650.6	68.6	25.9
375.39	4.235	656.7	66.8	23.8
375.40	4.244	661.6	64.5	21.1
375.42	4.265	671.6	60.8	16.9
375.43	4.280	678.0	59.6	15.4
375.43	4.292	683.0	58.8	14.3
375.45	4.349	701.4	56.7	11.1
375.46	4.473	729.6	55.5	8.1
375.46	4.527	739.0	55.0	7.1
375.46	4.625	753.3	55.0	6.1
375.46	4.681	760.3	55.2	5.9
375.18	4.942	790.8	55.9	4.6

Table 7. Thermal Conductivity of HFC-134a along the Quasi-Isotherm 375.72 K

T / K	p / MPa	ρ / kg·m^{-3}	λ / mW·m^{-1}·K^{-1}	$\Delta\lambda_c$ / mW·m^{-1}·K^{-1}
376.61	3.210	163.3	24.4	0.3
376.60	3.210	163.4	24.6	0.5
376.59	3.210	163.4	24.8	0.7
376.56	3.210	163.4	25.7	1.6
376.55	3.302	172.4	26.3	1.9
376.53	3.468	190.4	26.9	2.0
376.51	3.504	194.8	27.5	2.5
376.50	3.593	206.2	28.1	2.8
376.48	3.675	217.9	28.8	3.1
376.46	3.783	235.6	29.7	3.5
376.44	3.783	235.7	30.3	4.1
376.42	3.872	253.1	31.5	4.8
376.41	3.872	253.2	31.7	5.0
376.40	3.872	253.3	32.3	5.6
376.11	3.913	265.2	33.3	6.3
376.10	3.941	272.5	34.2	7.0
376.08	3.975	282.4	35.2	7.7
376.06	4.011	294.3	36.2	8.3
376.04	4.039	305.0	37.9	9.7
375.99	4.072	320.6	41.7	13.0
375.92	4.120	352.4	48.5	18.8
375.87	4.132	365.3	54.8	24.7
375.83	4.141	377.5	60.0	29.4
375.80	4.150	391.9	65.6	34.5
375.77	4.161	415.1	73.1	41.1
375.76	4.161	416.6	75.2	43.2
375.72	4.178	479.0	85.7	51.3
375.73	4.179	479.9	83.0	48.5
375.72	4.187	516.7	88.1	52.0
375.73	4.199	557.7	84.1	46.1
375.74	4.210	584.4	79.9	40.7
375.76	4.223	604.9	75.2	35.0
375.79	4.241	624.3	67.3	26.0
375.82	4.254	634.0	62.7	20.9
375.84	4.279	651.4	58.9	16.2
375.85	4.296	660.9	57.3	14.0
375.86	4.316	670.4	55.8	12.0
375.86	4.334	678.3	55.1	10.8
375.87	4.349	683.6	54.6	10.0
375.87	4.363	688.6	53.9	9.0
375.88	4.387	695.9	53.5	8.1
375.88	4.432	708.2	52.6	6.5
375.89	4.451	712.4	52.1	5.8
375.88	4.461	715.0	52.6	6.1
375.88	4.461	715.0	52.4	5.9
375.89	4.630	744.7	52.0	3.7
376.16	4.754	755.6	52.3	3.2
376.15	4.789	759.9	52.7	3.3
376.15	5.037	784.4	52.9	2.0
376.15	5.092	788.9	53.1	1.9
376.15	5.216	798.4	53.4	1.4
376.15	5.296	803.9	53.6	1.3
376.14	5.520	818.0	54.0	0.8
376.14	5.651	825.3	54.3	0.5
376.14	5.740	830.0	54.5	0.4

the critical isochore, eq 8 can be also written as the following approximated form.[20]

$$\Delta\lambda_c = R_D \frac{k_B T}{6\pi\eta\xi} \rho C_p^c \tag{9}$$

where C_p^c is defined as the specific heat difference $C_p^c = C_p - C_v$. This latter critical property can be then calculated from the isothermal compressibility κ_T by using the thermodynamic relation

$$C_p^c = C_p - C_v = \left(\frac{T}{\rho}\right)\left(\frac{\partial p}{\partial T}\right)_\rho^2 \kappa_T \tag{10}$$

On the other hand, it was found that along the critical isochore over an extended temperature range of any pure fluid[21] the rescaled isothermal compressibility χ_T^*

$$\chi_T^* = \kappa_T p_c Z_c \tag{11}$$

lies on a single curve when it is plotted as a function of the rescaled temperature

$$\tau = Y_c t \tag{12}$$

where

$$t = \frac{T - T_c}{T_c} \tag{13}$$

is the usual reduced temperature distance to T_c. In eqs 11 and 12

$$Z_c = \frac{m_p p_c}{k_B T_c \rho_c} \tag{14}$$

where m_p is the molecular mass and k_B is the Boltzmann constant and

$$Y_c = \left[\left(\frac{\partial p}{\partial T}\right)_{\rho_c,T_c}\left(\frac{T_c}{p_c}\right)\right] - 1 \tag{15}$$

$(\partial p/\partial T)_{\rho_c,T_c}$ is the slope of the critical isochore line at the critical point. $\kappa_T^* = \kappa_T p_c$ is the usual reduced form of the isothermal compressibility. A similar analysis[21] has also shown that the rescaled correlation length

Table 8. Thermal Conductivity of HFC-134a along the Quasi-Isotherm 376.02 K

T / K	p / MPa	ρ / kg·m^{-3}	λ / mW·m^{-1}·K^{-1}	$\Delta\lambda_c$ / mW·m^{-1}·K^{-1}
376.98	3.510	194.0	27.4	2.3
376.95	3.650	212.2	28.5	3.0
376.92	3.740	225.8	29.5	3.6
376.90	3.800	235.9	30.4	4.2
376.87	3.880	251.3	31.8	5.1
376.81	3.990	277.7	34.6	7.0
376.78	4.040	292.9	36.4	8.4
376.73	4.100	316.3	39.5	10.8
376.69	4.140	337.1	42.7	13.2
376.21	4.150	363.3	48.0	17.9
376.19	4.160	374.0	50.3	19.7
376.10	4.180	408.5	62.2	30.4
376.07	4.190	433.5	69.3	36.7
376.05	4.198	459.6	75.4	41.7
376.04	4.200	468.3	78.4	44.4
376.03	4.203	481.0	80.7	46.2
376.02	4.205	490.7	81.7	46.7
376.02	4.207	497.7	82.2	46.9
376.02	4.209	504.7	82.6	47.1
376.02	4.213	518.6	82.6	46.5
376.02	4.217	531.9	82.1	45.3
376.03	4.222	544.7	80.6	43.3
376.03	4.225	553.3	79.7	41.9
376.04	4.230	564.0	77.4	39.2
376.04	4.233	571.2	76.6	38.0
376.06	4.242	585.9	73.7	34.3
376.07	4.250	598.0	70.8	30.8
376.08	4.260	610.6	68.6	28.0
376.09	4.270	621.0	66.9	25.8
376.09	4.280	630.8	65.6	24.0
376.10	4.300	645.6	63.8	21.3
376.11	4.320	657.3	62.4	19.3
376.26	4.360	668.4	60.8	17.0
376.26	4.390	680.6	60.0	15.5
376.54	4.470	694.8	59.0	13.7
376.54	4.580	720.4	58.6	11.7
376.68	4.680	734.3	58.3	10.6
376.82	4.820	750.8	57.7	8.9
376.82	4.860	755.6	57.5	8.4

$$\xi^* = \xi/a \tag{16}$$

where

$$a = \left(\frac{k_B T_c}{p_c}\right)^{1/3} \tag{17}$$

is a single function of τ. Consequently, from eq 9, the rescaled quantity[22]

$$R_c^* = \frac{R_D \chi_T^*}{6\pi\xi^*} = \frac{\Delta\lambda_c \eta}{k_B (T(\partial P/\partial T)_{\rho_c})^2} P_c Z_c a \tag{18}$$

should be also a single function of τ. The validity of eq 18 along the critical isochore can be controlled in the R134a case by using the critical parameters of eq 1 and $(\partial p/\partial T)_{\rho_c,T_c} = 0.0831$ MPa·K^{-1}. The critical enhancement of the thermal conductivity data and the shear viscosity data are given in columns 2 and 3 of Table 18, respectively. The values of $\Delta\lambda_c$ were calculated at each temperature value reported in column 1 of Table 18, by interpolating at the critical density the values of the experimental data measured at the closest density of ρ_c. The values of η at each temperature were obtained from the NIST Tables[23] for ρ

Table 9. Thermal Conductivity of HFC-134a along the Quasi-Isotherm 376.27 K

T / K	p / MPa	ρ / kg·m^{-3}	λ / mW·m^{-1}·K^{-1}	$\Delta\lambda_c$ / mW·m^{-1}·K^{-1}
376.87	4.101	313.7	45.2	16.7
376.82	4.117	321.8	47.0	18.2
376.68	4.141	338.0	52.4	23.0
376.65	4.147	342.6	54.5	25.0
376.61	4.150	345.9	56.2	26.6
376.58	4.158	352.6	57.9	28.1
376.55	4.165	359.1	59.8	29.7
376.51	4.168	363.5	61.8	31.6
376.48	4.174	370.4	63.9	33.5
376.44	4.178	376.7	66.1	35.5
376.41	4.184	385.4	68.4	37.5
376.38	4.192	398.1	71.2	39.8
376.34	4.199	413.3	74.0	42.0
376.31	4.210	440.0	77.0	44.1
376.29	4.214	453.7	78.0	44.5
376.28	4.218	466.9	78.9	44.9
376.27	4.230	535.1	81.1	44.2
376.26	4.264	590.0	81.0	41.4
376.28	4.267	591.7	80.3	40.6
376.29	4.279	607.2	78.6	38.2
376.34	4.305	628.8	74.6	33.0
376.44	4.354	654.7	66.3	23.2
376.52	4.404	673.6	61.2	17.1
376.57	4.451	688.0	58.7	13.7
376.87	4.504	692.2	57.1	11.9
376.89	4.548	703.0	56.2	10.3
377.73	4.701	711.3	55.0	8.6
377.93	4.800	724.0	54.7	7.5
377.93	4.851	731.9	54.7	7.0
377.86	4.997	752.3	54.8	5.8
378.11	5.504	793.3	56.0	4.2
377.96	6.000	824.4	56.9	3.0
378.07	6.502	846.1	58.0	2.5
378.05	7.003	864.9	58.9	2.1
378.18	7.450	878.2	59.7	1.8
378.16	8.004	893.9	60.5	1.5
378.29	8.408	903.3	61.2	1.4
378.27	9.008	917.1	62.0	1.1
378.26	9.506	927.5	62.7	1.0
378.25	9.919	935.4	63.2	0.9
378.24	10.507	946.0	64.0	0.8
378.37	10.981	953.2	64.6	0.8
378.36	11.376	959.5	65.0	0.7
378.34	12.420	974.7	66.3	0.7
378.33	13.441	988.1	67.4	0.6
378.31	14.505	1000.8	68.3	0.5
378.29	16.500	1021.8	70.1	0.4
378.27	18.500	1040.2	71.6	0.2
378.25	21.005	1060.4	73.6	0.2

Table 10. Thermal Conductivity of HFC-134a along the Quasi-Isotherm 377.01 K

T / K	p / MPa	ρ / kg·m^{-3}	λ / mW·m^{-1}·K^{-1}	$\Delta\lambda_c$ / mW·m^{-1}·K^{-1}
377.58	4.079	293.7	36.6	8.5
377.55	4.126	310.3	39.0	10.4
377.51	4.164	327.1	41.5	12.5
377.32	4.211	359.9	46.6	16.5
377.29	4.226	372.9	49.4	18.8
377.27	4.235	382.2	51.3	20.4
377.26	4.241	388.7	52.9	21.8
377.24	4.249	399.0	55.5	24.0
377.19	4.266	426.9	63.0	30.5
377.18	4.270	434.6	64.8	32.0
377.17	4.275	444.7	67.1	33.9
377.01	4.289	499.9	72.0	36.6
377.01	4.294	511.1	72.4	36.5
377.01	4.307	538.7	72.4	35.2
377.01	4.309	542.6	72.0	34.7
377.01	4.312	548.4	71.7	34.1
377.02	4.322	564.6	70.6	32.2
377.02	4.332	580.1	69.1	30.0
377.03	4.343	593.4	67.4	27.6
377.04	4.356	606.8	66.1	25.6
377.05	4.380	627.0	63.6	22.1
377.05	4.384	630.0	63.4	21.7
377.06	4.397	638.1	62.5	20.4
377.06	4.417	649.8	61.7	18.9
377.07	4.439	660.1	60.6	17.2
377.07	4.473	674.0	60.0	15.9
377.08	4.495	681.2	59.5	14.9
377.08	4.538	694.0	58.7	13.4
377.36	4.613	703.3	58.3	12.4
377.36	4.653	712.0	57.8	11.4
377.36	4.697	720.4	57.8	10.9
377.36	4.760	731.0	57.6	10.0
377.37	4.836	741.8	56.9	8.7
377.37	4.907	750.8	56.2	7.4

Table 11. Thermal Conductivity of HFC-134a along the Quasi-Isotherm 377.83 K

T / K	p / MPa	ρ / kg·m^{-3}	λ / mW·m^{-1}·K^{-1}	$\Delta\lambda_c$ / mW·m^{-1}·K^{-1}
379.10	4.331	369.9	44.1	13.5
377.97	4.302	404.5	48.7	18.0
377.95	4.301	404.9	50.3	18.5
377.93	4.309	415.6	52.1	19.9
377.91	4.321	432.9	55.7	22.8
377.89	4.330	448.2	58.3	24.9
377.87	4.339	464.8	61.7	27.6
377.85	4.351	487.7	65.2	30.2
377.84	4.360	504.5	66.8	31.1
377.83	4.369	521.1	67.8	31.4
377.83	4.381	540.2	68.1	30.8
377.83	4.390	553.5	68.1	30.2
377.83	4.400	567.0	67.8	29.2
377.84	4.411	579.2	66.8	27.6
377.84	4.420	589.1	65.8	26.2
377.85	4.432	599.8	65.2	25.0
377.85	4.441	607.7	64.0	23.4
377.86	4.451	614.9	63.1	22.1
377.86	4.460	621.5	62.3	20.9
377.87	4.470	627.4	61.4	19.8
377.87	4.479	633.0	60.6	18.7
378.02	4.500	635.5	60.1	18.0
377.89	4.518	652.1	58.7	15.8
377.89	4.531	657.7	58.2	14.9
377.90	4.541	661.3	57.5	14.0
377.90	4.551	665.2	57.0	13.3
377.90	4.561	668.8	56.6	12.6
377.90	4.582	675.9	56.3	12.0

Table 12. Thermal Conductivity of HFC-134a along the Quasi-Isotherm 378.25 K

T / K	p / MPa	ρ / kg·m^{-3}	λ / mW·m^{-1}·K^{-1}	$\Delta\lambda_c$ / mW·m^{-1}·K^{-1}
378.90	3.950	250.2	31.7	4.9
378.85	4.050	271.4	33.9	6.5
378.83	4.090	281.3	35.1	7.3
378.81	4.120	289.5	36.0	8.0
378.54	4.130	295.9	36.4	8.2
378.53	4.140	299.1	36.8	8.5
378.53	4.150	302.3	37.1	8.7
378.50	4.180	313.1	38.5	9.8
378.49	4.200	320.9	39.5	10.6
378.47	4.220	329.7	40.8	11.5
378.45	4.240	339.5	42.2	12.6
378.43	4.260	350.6	43.8	13.9
378.41	4.280	363.4	46.1	15.7
378.40	4.290	370.5	47.2	16.6
378.38	4.300	378.8	48.8	17.9
378.36	4.310	388.0	50.6	19.4
378.35	4.320	397.5	52.4	20.8
378.33	4.330	408.8	54.7	22.7
378.31	4.340	421.3	57.0	24.6
378.29	4.350	435.4	59.7	26.8
378.28	4.360	449.9	62.2	28.7
378.27	4.370	465.4	64.5	30.4
378.26	4.380	481.7	65.7	31.0
378.26	4.390	497.0	66.4	30.9
378.25	4.395	506.0	66.7	30.9
378.25	4.400	513.5	66.7	30.6
378.26	4.410	527.0	66.7	30.0
378.26	4.420	541.0	66.1	28.7
378.26	4.430	554.1	65.5	27.5
378.27	4.440	565.1	64.5	26.0
378.27	4.450	576.2	63.9	24.9
378.27	4.460	586.4	63.3	23.8
378.28	4.470	594.7	62.5	22.5
378.28	4.480	603.2	61.6	21.2
378.29	4.490	610.1	61.1	20.3
378.29	4.500	617.2	60.8	19.7
378.29	4.510	623.8	60.3	18.8
378.29	4.520	629.8	60.1	18.2
378.29	4.530	635.4	59.8	17.7
378.30	4.540	640.0	59.5	17.2
378.30	4.550	644.9	59.3	16.6
378.30	4.570	653.8	58.8	15.6
378.30	4.590	661.7	58.5	14.9
378.31	4.620	671.7	58.1	13.9
378.31	4.626	673.6	57.8	13.6
378.31	4.650	680.9	57.3	12.7
378.31	4.688	691.0	57.1	11.8
378.31	4.730	700.7	56.9	11.1
378.32	4.770	708.7	56.7	10.4
378.59	4.860	718.1	56.5	9.6
378.59	4.900	724.6	56.5	9.2

Table 13. Thermal Conductivity of HFC-134a along the Quasi-Isotherm 379.09 K

T / K	p / MPa	ρ / kg·m^{-3}	λ / mW·m^{-1}·K^{-1}	$\Delta\lambda_c$ / mW·m^{-1}·K^{-1}
379.50	4.165	293.4	35.5	7.4
379.50	4.175	296.2	35.8	7.6
379.48	4.200	304.0	36.7	8.2
379.47	4.224	311.9	37.6	8.9
379.45	4.254	322.9	38.9	9.8
379.43	4.282	334.6	40.5	11.0
379.42	4.288	337.5	40.8	11.2
379.40	4.309	347.8	42.2	12.3
379.40	4.317	351.8	42.7	12.7
379.39	4.330	359.1	43.7	13.4
379.37	4.346	369.2	45.3	14.7
379.36	4.355	375.3	46.2	15.4
379.34	4.369	385.8	47.8	16.6
379.33	4.376	391.5	48.7	17.3
379.32	4.386	400.0	50.1	18.4
379.30	4.396	409.7	51.6	19.5
379.29	4.404	417.7	53.0	20.6
379.28	4.414	428.3	54.5	21.7
379.27	4.424	439.6	55.9	22.7
379.26	4.431	448.2	57.3	23.8
379.25	4.442	461.8	59.3	25.2
379.23	4.452	475.7	60.8	26.2
379.23	4.453	476.9	61.4	26.7
379.09	4.452	489.5	62.5	27.3
379.09	4.460	499.6	62.7	27.1
379.09	4.464	504.6	63.0	27.2
379.09	4.470	512.0	63.0	26.9
379.09	4.475	518.2	63.0	26.6
379.09	4.484	528.9	63.0	26.1
379.22	4.504	538.6	62.8	25.5
379.09	4.500	547.0	62.7	25.0
379.23	4.520	554.5	62.0	23.9
379.23	4.530	564.3	61.5	22.9
379.24	4.540	572.6	60.9	21.9
379.24	4.547	578.7	60.6	21.4
379.24	4.560	589.3	60.1	20.3
379.24	4.570	596.7	59.9	19.7
379.25	4.600	615.6	59.1	17.9
379.25	4.620	626.7	58.7	16.9
379.25	4.642	637.3	58.4	16.1
379.26	4.662	645.5	57.9	15.2
379.26	4.680	652.5	57.7	14.6
379.26	4.703	660.7	57.5	13.9
379.26	4.739	672.0	57.3	13.0
379.26	4.766	679.5	57.3	12.6
379.26	4.806	689.4	57.0	11.8
379.40	4.838	692.4	56.7	11.2
379.40	4.888	702.7	56.2	10.2
379.41	4.932	710.5	55.8	9.3
379.41	5.000	721.6	55.4	8.2
379.41	5.051	729.0	55.0	7.3

$= \rho_c$. The corresponding calculated values of R_c^* in the rescaled temperature range ($2.6 \cdot 10^{-3} < \tau = Y_c((T - T_c)/T_c) < 5 \cdot 10^{-1}$) covered by the experiments are shown in column 4 of Table 18. The fit of the complete data set by an effective pure power law with adjustable exponent and adjustable amplitude gives $R_c^* = 0.0164\tau^{-0.6162}$. We have then eliminated in the following fitting procedures the data point corresponding to the closest temperature distance to T_c, due to the large uncertainty in our estimation of $\Delta\lambda_c$ at $\rho = \rho_c$ and $T = 374.26$ K. The best fit of the remaining data set of R_c^*, was thus

$$R_c^* = 0.01441\tau^{-0.6703} \qquad (19)$$

The latter power law compares favorably (deviations lower than 2 %) with the single power law $R_c^* = 0.0139\tau^{-0.655}$ given in ref 22, which was obtained in a similar rescaled temperature range by the analysis of 14 other pure fluids. The calculated values of R_c^* by using eq 19 are given in column 5 of Table 18. The residuals are lower than 5 % with the present experimental estimation of this quantity (except the 25 % residual of the eliminated point). The equivalent best fit of the critical thermal conductivity enhancement in the reduced temperature range ($4.3 \cdot 10^{-4} < t = ((T - T_c)/T_c) < 8 \cdot 10^{-2}$) gives

$$\Delta\lambda_c \text{ (mW·m}^{-1}\text{·K}^{-1}) = 1.5742t^{-0.6437} \qquad (20)$$

In eqs 19 and 20, the effective values (0.6703 and 0.6437, respectively) of the critical exponents are significantly different from their expected asymptotic Ising values (0.61 and 0.57, respectively). As already noted in ref 22, these non-Ising values of the exponent means that the experimental data obtained in our present temperature range can be described only accounting for the classical-to-critical crossover theories. An alternative empirical approach consists thus to explicit directly the effective pure power laws that are only valid in this restricted temperature

Table 14. Thermal Conductivity of HFC-134a along the Quasi-Isotherm 381.53 K

T / K	p / MPa	ρ / kg·m^{-3}	λ / mW·m^{-1}·K^{-1}	$\Delta\lambda_c$ / mW·m^{-1}·K^{-1}
381.63	4.490	373.9	46.4	15.4
381.63	4.500	379.1	47.2	16.0
381.63	4.500	379.1	46.8	15.7
381.62	4.510	384.9	47.8	16.4
381.61	4.516	388.6	48.3	16.8
381.61	4.520	390.9	48.7	17.1
381.61	4.525	393.8	49.0	17.3
381.60	4.530	397.2	49.5	17.7
381.58	4.569	423.8	51.8	19.0
381.56	4.600	448.0	53.6	19.9
381.55	4.612	458.1	54.2	20.1
381.53	4.627	471.5	55.1	20.4
381.53	4.640	482.1	55.5	20.4
381.53	4.650	490.4	56.0	20.5
381.53	4.660	498.6	56.2	20.4
381.53	4.670	506.7	56.5	20.3
381.53	4.680	514.7	56.5	20.0
381.54	4.700	529.5	56.2	19.1
381.54	4.760	571.0	56.0	16.9
381.55	4.780	582.3	55.8	16.1
381.55	4.800	593.2	55.5	15.3
381.55	4.815	600.8	55.3	14.7
381.56	4.830	607.4	55.1	14.2
381.56	4.860	620.5	54.9	13.3
381.56	4.900	635.6	54.2	11.8
381.56	4.920	642.3	54.2	11.4
381.56	4.950	651.6	54.3	11.0
381.56	4.982	660.6	54.3	10.5
381.56	5.016	669.2	54.3	10.0
381.56	5.068	680.9	54.3	9.4
381.57	5.092	685.6	53.9	8.7
381.57	5.125	691.9	53.8	8.2
381.57	5.136	693.9	53.8	8.1
381.57	5.169	699.7	53.6	7.5
381.57	5.201	705.0	53.6	7.2

range. That allows us to obtain more easily each "theoretical" power law which is equivalent to the experimental power law of eq 20, in conformity with the single power law that governs the master behavior of eq 18 for any pure fluid. In the following, we illustrate this "theoretical" estimation of $\Delta\lambda_c$ when we assume that the knowledge of the specific heat data and the correlation length data replace the knowledge of the isothermal compressibility and the slope of the critical isochore in our experimental temperature range. We have thus rewritten eq 18 as follows

$$\Delta\lambda_c = R_{D,eff}\frac{k_B T}{6\pi\eta\xi}\rho_c(C_p - C_v) \quad (21)$$

In eq 21, we have introduced an effective amplitude term $R_{D,eff}$ to account for the effective values of the exponents that describe the observed temperature behavior of η, $C_p - C_V$, and ξ along the critical isochore. The viscosity data calculated from NIST tables[23] (column 3, Table 18) were fit by the linear equation $\eta(\mu Pa\cdot s^{-1}) = 34.686\,(1 + 0.4731t)$ in agreement with a small singular behavior of this transport property (which can be neglected in our temperature range). From the values of C_p and C_v given in columns 6 and 7 of Table 18, respectively, the values of $\rho_c(C_p - C_V)$ were fit by the power law equation $\rho_c(C_p - C_V)$ (kJ·m^{-3}·K^{-1}) = $73.161t^{-1.03222}$. In the absence of measurements of the correlation length of R134a, we have assumed that the theoretical estimation[24,25] of the leading Ising power law $\xi = \xi_0 t^{-0.63}$, with $\xi_0 = 1.8785\cdot10^{-10}$ m,[22] remains valid in our experimental range. Accordingly, the fit of the prefactor term $R_{D,eff}$ leads to the following power law

$$R_{D,eff} = 0.4859t^{-0.25057} \quad (22)$$

Introducing all these previous temperature behaviors in eq 21, the "theoretical" power law equation of the critical enhancement of the thermal conductivity reads as follows

$$\Delta\lambda_c\,(mW\cdot m^{-1}\cdot K^{-1}) = 1.4954\frac{1+t}{1+0.4731t}t^{-0.6528} \quad (23)$$

The small difference of the exponent values in eqs 20 and 23 is due to the small explicit linear temperature dependences of eq 23. The calculated values of $\Delta\lambda_c$ by using eq 23 (column 8, Table 18) compare favorably with the experimental values (column 2, Table 18) and with the calculated values using

Table 15. Thermal Conductivity of HFC-134a along the Quasi-Isotherm 385.18 K

T / K	p / MPa	ρ / kg·m^{-3}	λ / mW·m^{-1}·K^{-1}	$\Delta\lambda_c$ / mW·m^{-1}·K^{-1}
385.78	3.920	213.2	29.3	2.9
385.75	4.060	230.5	30.5	3.6
385.61	4.120	239.3	31.1	4.0
385.59	4.200	251.1	32.0	4.6
385.57	4.260	260.7	32.8	5.1
385.42	4.310	270.2	33.5	5.5
385.41	4.360	279.5	34.3	6.0
385.39	4.410	289.6	35.2	6.6
385.37	4.460	300.5	36.3	7.4
385.36	4.500	309.8	37.1	7.9
385.34	4.540	320.1	38.2	8.6
385.33	4.580	331.0	39.3	9.4
385.31	4.610	340.1	40.1	9.9
385.30	4.640	349.6	41.1	10.6
385.29	4.670	359.8	42.1	11.3
385.28	4.700	370.7	43.1	11.8
385.26	4.730	382.7	44.6	12.9
385.25	4.760	395.3	45.8	13.7
385.23	4.800	413.8	47.1	14.4
385.22	4.820	423.6	48.0	14.8
385.21	4.840	433.8	48.8	15.3
385.20	4.880	454.7	50.5	16.1
385.19	4.900	465.6	51.2	16.5
385.19	4.918	475.2	51.8	16.6
385.18	4.940	487.3	52.2	16.5
385.18	4.959	497.3	52.6	16.5
385.18	4.978	507.2	52.8	16.3
385.18	5.000	518.5	53.0	16.0
385.18	5.022	529.4	53.0	15.5
385.18	5.042	539.0	53.0	15.1
385.18	5.058	546.4	53.0	14.7
385.18	5.080	556.3	53.0	14.3
385.18	5.100	564.8	53.0	13.9
385.18	5.120	573.0	53.0	13.5
385.18	5.151	585.0	52.8	12.7
385.18	5.179	595.1	52.6	11.9
385.18	5.224	609.8	52.4	11.0
385.18	5.254	618.8	52.2	10.3
385.19	5.296	630.1	51.8	9.3
385.19	5.322	636.7	51.8	9.0
385.19	5.358	645.3	51.6	8.3
385.19	5.402	654.9	51.6	7.8
385.19	5.454	665.3	51.4	7.0
385.19	5.513	675.9	51.2	6.2
385.72	5.700	693.8	51.4	5.3
385.72	5.714	695.7	51.6	5.4
387.25	6.371	740.5	52.7	3.6
387.23	6.650	761.5	53.6	3.1
387.22	7.002	783.2	54.5	2.7
387.20	7.501	808.2	55.9	2.3
387.19	7.800	820.9	56.4	1.9
387.30	8.468	844.2	57.8	1.7
387.27	9.502	874.3	59.7	1.3
387.37	11.008	907.7	61.9	0.9
387.37	11.503	917.1	62.5	0.8
387.34	13.000	942.4	64.2	0.5
387.33	13.500	949.9	64.8	0.5
387.33	14.002	957.1	65.3	0.4
387.32	14.910	969.1	66.3	0.3
387.30	16.290	985.7	67.6	0.3
387.29	17.000	993.6	68.2	0.1
387.28	18.006	1004.0	69.1	0.1

Table 16. Thermal Conductivity of HFC-134a along the Quasi-Isotherm 394.47 K

T / K	p / MPa	ρ / kg·m^{-3}	λ / mW·m^{-1}·K^{-1}	$\Delta\lambda_c$ / mW·m^{-1}·K^{-1}
395.24	4.405	234.9	30.9	3.0
395.23	4.495	245.1	31.5	3.4
394.95	4.583	256.9	32.2	3.7
394.94	4.649	265.5	32.8	4.1
394.93	4.722	275.4	33.5	4.5
394.91	4.821	289.8	34.6	5.1
394.89	4.890	300.6	35.3	5.5
394.88	4.950	310.5	36.0	5.9
394.88	4.978	315.3	36.3	6.1
394.60	5.055	331.7	37.4	6.6
394.57	5.176	356.2	39.0	7.4
394.56	5.246	371.5	40.0	8.0
394.55	5.300	384.1	40.9	8.4
394.54	5.314	387.6	41.1	8.5
394.53	5.366	400.3	41.9	8.8
394.52	5.428	416.2	43.0	9.3
394.50	5.527	442.6	44.4	9.7
394.49	5.583	457.9	45.3	10.0
394.49	5.626	469.5	45.7	10.0
394.49	5.641	473.6	46.0	10.1
394.47	5.760	505.6	47.2	9.9
394.47	5.767	507.5	47.2	9.8
394.47	5.800	515.9	47.6	9.9
394.47	5.811	518.7	47.6	9.8
394.47	5.851	528.6	48.0	9.7
394.47	5.886	537.1	48.0	9.3
394.46	5.940	549.9	48.3	9.1
394.46	5.980	558.9	48.7	9.0
394.46	6.044	572.5	49.1	8.7
394.46	6.100	583.8	49.2	8.3
394.45	6.140	591.6	49.4	8.1
394.45	6.200	602.5	49.6	7.7
394.45	6.260	612.8	49.8	7.4
394.45	6.300	619.3	50.0	7.2
394.45	6.399	634.2	50.3	6.8
394.44	6.457	642.5	50.7	6.7
394.44	6.523	651.2	50.9	6.5
394.44	6.557	655.5	51.1	6.4
394.57	6.665	665.1	51.3	6.1
394.57	6.720	672.4	51.5	5.9
394.57	6.754	676.0	51.5	5.7
394.57	6.800	680.8	51.5	5.4
394.56	6.908	691.5	51.9	5.2
394.56	7.067	705.6	52.3	4.7
394.69	7.159	711.5	52.6	4.7
394.69	7.321	723.8	52.8	4.1
394.68	7.457	733.4	53.3	3.9
394.68	7.521	737.6	53.5	3.9
394.68	7.635	744.8	53.7	3.6
394.81	7.706	747.8	53.8	3.6
394.81	7.827	754.8	54.1	3.4

eq 20, except for the closest temperature to T_c. It is essential to note that a similar approach that starts with the single power law $R_c^* = 0.0139\tau^{-0.655}$ of ref 21 in place of our above eq 19 also provides eq 23 with only minor differences in the values of the effective amplitude and the effective exponent.

To calculate $\Delta\lambda_c$ outside the critical isochore, we have then generalized eq 21 as the following form

$$\Delta\lambda_c(t,\Delta\rho^*) = R_{D,\mathrm{eff}}(t,\Delta\rho^*)\frac{k_B T}{6\pi\eta(t,\Delta\rho^*)\xi(t,\Delta\rho^*)} \times \rho[C_p(t,\Delta\rho^*) - C_v(t,\Delta\rho^*)] \quad (24)$$

where the temperature and density dependences of the different quantities are accounted for introducing the reduced quantity t of eq 13 and the reduced density difference

$$\Delta\rho^* = \frac{\rho - \rho_c}{\rho_c} \quad (25)$$

Now the effective function $R_{D,\mathrm{eff}}(t, \Delta\rho^*)$ is an empirical function which characterizes our extended temperature and density range measured by t and $\Delta\rho^*$. Equation 24 is then similar to the crossover semiempirical equation $\Delta\lambda_c = R_D[(k_B T)/(6\pi\eta\xi)]\rho C_p^c F(t, \Delta\rho^*)$ proposed by Hanley et al. in ref 20 where $F(t, \Delta\rho^*)$ is an empirical damping function used in their extended critical region.

The values of $C_p(t, \Delta\rho^*)$, $C_v(t, \Delta\rho^*)$ are calculated from the equation of state[5] and $\eta(t, \Delta\rho^*)$ from the NIST tabulated

Table 17. Thermal Conductivity of HFC-134a along the Quasi-Isotherm 404.36 K

T / K	p / MPa	ρ / kg·m^{-3}	λ / mW·m^{-1}·K^{-1}	$\Delta\lambda_c$ / mW·m^{-1}·K^{-1}
406.09	1.196	39.3	23.6	0.0
405.81	1.930	67.5	24.3	0.0
405.27	2.343	85.3	24.7	0.0
405.26	2.524	93.6	24.9	0.0
405.25	2.700	101.9	25.2	0.1
405.25	2.863	109.9	25.4	0.1
405.34	3.411	139.4	26.4	0.3
405.07	3.698	157.1	27.1	0.5
405.06	3.790	163.0	27.4	0.6
405.05	3.914	171.3	27.8	0.8
404.77	4.070	182.6	28.3	1.0
404.76	4.201	192.3	28.7	1.2
404.76	4.278	198.2	29.0	1.4
404.73	4.451	212.2	29.8	1.7
404.73	4.467	213.5	29.8	1.7
404.73	4.523	218.2	30.1	1.8
404.71	4.641	228.6	30.7	2.1
404.70	4.754	240.1	31.2	2.4
404.68	4.909	254.4	32.1	2.8
404.67	5.039	268.0	32.9	3.2
404.65	5.162	281.7	33.6	3.5
404.51	5.242	291.8	34.2	3.8
404.50	5.330	302.6	34.9	4.1
404.49	5.419	314.0	35.5	4.4
404.48	5.494	324.1	36.1	4.7
404.47	5.579	335.9	36.8	5.0
404.46	5.668	348.9	37.5	5.3
404.45	5.750	361.3	38.3	5.7
404.44	5.814	371.3	38.8	5.9
404.43	5.860	378.7	39.3	6.1
404.43	5.908	386.4	39.6	6.1
404.42	5.967	396.2	40.2	6.4
404.40	6.039	408.5	41.0	6.7
404.40	6.080	415.4	41.3	6.7
404.38	6.342	461.1	43.3	7.0
404.34	6.434	477.5	44.0	7.0
404.34	6.516	491.5	44.6	7.0
404.36	6.559	498.4	44.9	7.0
404.36	6.640	511.7	45.3	6.9
404.23	6.723	526.8	46.0	6.9
404.23	6.754	531.6	46.1	6.8
403.83	6.852	552.1	46.8	6.6
403.82	6.973	569.4	47.5	6.4
403.69	7.105	588.6	48.0	6.0
403.68	7.203	600.8	48.4	5.8
405.49	7.506	611.9	49.0	5.6
403.69	7.364	619.0	49.0	5.4
405.48	7.814	642.0	49.9	4.9
405.47	8.558	697.9	51.5	3.4
405.46	8.835	714.6	52.1	3.0
407.01	10.638	782.0	55.7	2.1
407.00	10.911	791.2	56.2	1.9
406.99	11.426	807.2	56.9	1.6
406.96	12.915	845.6	59.1	1.1
406.94	13.921	866.9	60.3	0.7
406.93	14.350	875.1	60.8	0.6
406.91	15.679	898.1	62.3	0.3
406.90	16.345	908.5	63.0	0.3
406.88	18.500	938.0	65.2	0.1

Table 18. Variation of $\Delta\lambda_c$, η, R_c^*, C_p, and C_v as a Function of Temperature T along the Critical Isochore

T / K	$\Delta\lambda_c$(exp) / mW·m^{-1}·K^{-1}	η / μPa·s^{-1}	R_c^*(exp) / eq 18	R_c^* (cal) / eq 19	C_p / J/g·K	C_v / J/g·K	$\Delta\lambda_c$(cal) / mW·m^{-1}·K^{-1} eq 23
374.37	151.9	34.693	0.4534	0.7332	409.68	1.2403	236.66
374.96	89.7	34.719	0.2671	0.2603	87.058	1.2343	86.397
375.14	73.1	34.727	0.2175	0.2253	70.299	1.2325	75.097
375.28	64.1	34.733	0.1906	0.2051	61.17	1.2311	68.541
375.72	52.0	34.752	0.1544	0.1628	43.516	1.2268	54.773
376.02	47.5	34.766	0.1408	0.1442	36.407	1.2240	48.682
376.27	45.0	34.777	0.1333	0.1322	32.067	1.2217	44.755
377.01	36.6	34.809	0.1081	0.1077	23.769	1.2151	36.667
377.83	31.4	34.845	0.0924	0.0906	18.543	1.2081	31.042
378.25	30.9	34.863	0.0908	0.0842	16.689	1.2048	28.913
379.08	27.2	34.900	0.0797	0.0743	13.968	1.1983	25.622
381.53	20.5	35.005	0.05945	0.0565	9.5471	1.1815	19.704
385.18	16.5	35.167	0.0472	0.0431	6.6389	1.1612	15.206
394.47	10.0	35.575	0.02757	0.02857	3.9986	1.1279	10.314
404.36	7.3	36.008	0.01939	0.02189	3.002	1.1102	8.058

data.[23] The values of the correlation length $\xi(t, \Delta\rho^*)$ were calculated in terms of the cubic restricted model, i.e., $\xi(t, \Delta\rho^*) = \xi(r, \theta) = r^{-0.63}\xi_0^+ R(\theta)$,[26] as proposed by Sengers and Levelt-Sengers.[27] In the latter equation, the (r, θ) parameters are related to $(t, \Delta\rho^*)$ by $t = r(1 - b^2\theta^2)$ and $\Delta\rho^* = r^{0.325}k\theta(1 + c\theta^2)$, while $R(\theta) = 1 + 0.16\theta^2$.[26] The corresponding values of the model parameters are $b^2 \approx 1.2766$ and $c \approx 0.055$,[26] while the values $k = 1.1629$ and $a = 23.456$[27,28] of the two system-dependent parameters are obtained for the R134a case.[25,28] Then the functional form of $R_{D,eff}(t, \Delta\rho^*)$ was written as a product of three main contributions $R_{D,eff}(t, \Delta\rho^*) = R_{D,eff}(t)\cdot R_{S,eff}(|\Delta\rho^*|)\cdot R_{A,eff}(\Delta\rho^*)$, where the temperature contribution $R_{D,eff}(t)$ is accounted for by our previous eq 22, while the density contribution was split into a symmetrical function $R_{S,eff}(|\Delta\rho^*|)$ of the cubic equation

$$R_{S,eff}(|\Delta\rho^*|) = 16.0|\Delta\rho^*|^3 + 1 \quad (26)$$

and an asymmetrical function $R_{A,eff}(\Delta\rho^*)$ of the cubic equation

$$R_{A,eff}(\Delta\rho^*) = 0.9(\Delta\rho^*)^3 + 1 \quad (27)$$

Accordingly, the calculated values of the critical enhancement $\Delta\lambda_c$ of the thermal conductivity using eqs 24 to 27 are in satisfactory agreement (within the experimental uncertainty) with the experimental values calculated in the whole density range. As expected, we have observed that the residuals increase (overpassing then 50 %) only when $\Delta\lambda_c$ decrease significantly to reach a very small part of the total thermal conductivity (i.e., when the temperature and density distance to the critical point increase).

Finally, after estimation of the total thermal conductivity $\lambda(T, \rho)$ by using eqs 2, 4, 5, and 24, we have reported the related residuals $r_\lambda(\%) = 100\cdot(\lambda_{cal}/\lambda_{exp} - 1)$ (expressed in %) in Figure 2. The standard average deviation between the thermal conductivity calculated by eqs 2, 4, 5, and 24 and the experimental data is 4.5 % and reduces to 3.73 % when ignoring the isotherm 374.37 K closest to T_c. Though some more important deviations are observed between calculated and experimental values in limited density ranges, we estimate that they are mainly due to the fact that the experimental curves of the critical enhancement of the thermal conductivity and the tabulated values of $\rho_c(C_p - C_v)$ are not exactly symmetrical with respect to ρ_c.

Conclusion

New measurements of the thermal conductivity of HFC-134a are presented in the supercritical region, at temperatures from (370 to 405) K, along 15 quasi-isotherms and at pressures up to 40 MPa with an estimated uncertainty of ± 3 %. As expected, the (background + critical enhancement) additive form of the thermal conductivity data implies that the determination of the critical enhancement term is very sensitive to the analytical form of the background term. After a careful analysis of the temperature and density dependences of the background term, we have then shown that the magnitude of the critical enhancement is very large and follows a behavior which can be predicted from theory along the critical isochore. In this critical isochoric region, a correlation was developed to represent the variation of the thermal conductivity in terms of reduced parameters, which can be thus applied to any fluid. The variation of the thermal conductivity as a function of density was estimated by an empirical relation. The average deviations between calculated and experimental thermal conductivity data are less than 4.5 %, in the whole temperature range from (300 to 550) K and pressure range from (0.1 to 40) MPa. In the critical region, the temperature range is restricted to $T > T_c + 1$ K. However, to correlate the critical enhancement of R134a as a function of density in an extended critical region, a critical evaluation of other experimental data of R134a, reported in the literature, is necessary. Moreover, further comparisons with other fluids are required to develop a universal equation to represent the thermal

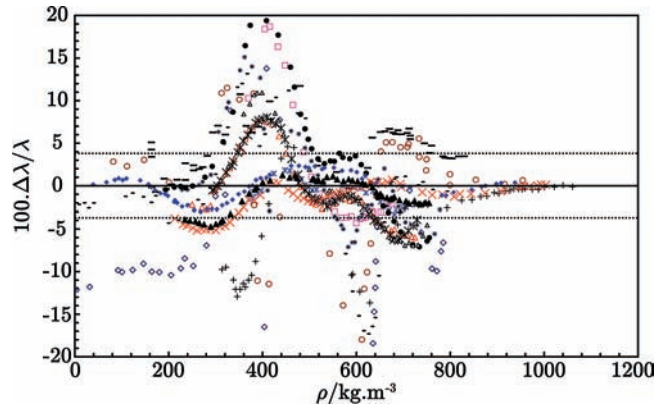

Figure 2. Fractional deviation $100\cdot\Delta\lambda/\lambda = 100\cdot[\lambda(\text{cal}) - \lambda(\text{exp})]/\lambda(\text{exp})$ of the thermal conductivity data of R134a, as a function of density. The calculated values are obtained using eqs 2, 4, 5, and 24 (see text for details). ◇, 374.37 K (not selected in the fitting procedure, see text); □, 377.83 K; △, 375.14K; ■, 381.53 K; *, 379.08 K; ○, 374.96 K; +, 375.14 K; -, 375.28 K; −, 375.72 K; ●, 376.02 K; +, 376.27; △, 377.01 K; ×, 385.18 K; ▲, 394.47 K; ◆, 404.36 K. The dashed-dotted lines are one standard deviation of the fit of our experimental data set of Tables 4 to 17.

conductivity of any fluid, in liquid and vapor states, including the extended critical region.

Literature Cited

(1) Le Neindre, B.; Garrabos, Y. Transport Properties of Refrigerants. *Rev. High Press. Sci. Technol.* **1998**, *7*, 1183–1188.

(2) Le Neindre B.; Garrabos Y. Transport Properties of Refrigerants. *Proc. Fifth Asian Thermophys. Prop. Conf.*; Kim, M. S., Ro, S. T. Eds.; (Seoul), 1998; p 415.

(3) Le Neindre, B.; Garrabos, Y. Measurements of the thermal conductivity of HFC-134a in the temperature range from 300 to 530 K and at pressures up to 50 MPa. *Int. J. Thermophys.* **1999**, *20*, 1379–1401.

(4) Le Neindre B.; Tufeu R. *Measurements of the thermal conductivity of fluids by the coaxial cylinder method, in: Experimental Thermodynamics*; Wakeham, W. A., Nagashima, A., Sengers, J. V., Eds.; Blackwell Scientific Publication, 1991; Vol. IV, pp 111−142.

(5) Tillner-Roth, R.; Baehr, H. D. An International Standard Formulation for the Thermodynamic Properties of 1,1,1,2-Tetrafluoroethane (HFC-134a) for Temperatures from 170 to 455 K and Pressure up to 70 MPa. *J. Phys. Chem. Ref. Data* **1994**, *23*, 657–729.

(6) Assael, M. J.; Nagasaka, Y.; Nieto de Castro, C. A.; Perkins, R. A.; Strom, K.; Vogel, E.; Wakeham, W. A. Status of the Round Robin on the Transport Properties of R134a. *Int. J. Thermophys.* **1995**, *16*, 63–78.

(7) Assael, M. J.; Karagiannidis, L.; Polimatldou, S. K. Measurements of the thermal conductivity of R22, R123, R134a, and R152a. *High Temp. High Press.* **1993**, *25*, 259–267.

(8) Kiselev, S. B.; Perkins, R. A.; Huber, M. L. Transport properties of refrigerants R32, R125, R134a, and R125 + R32 mixtures in and beyond the critical region. *Int. J. Refrig.* **1999**, *22*, 509–530.

(9) Perkins R. A.; Laesecke A.; Howley J.; Ramires M. L. V.; Gurova A. N.; Cusco L. Experimental thermal conductivity values for the IUPAC round-robin sample of 1,1,1,2-tetrafluoroethane (R134a). *Nat. Inst. Stand. Tech. Interagency Report 6605*, **2000**.

(10) Soldner, J.; Stephan, K. Measurement of thermal diffusivities with the photoacoustic effect. *Chem. Eng. Process.* **1999**, *38*, 585–591.

(11) Krauss, R.; Luettmer-Strathmann, J.; Sengers, J. V.; Stephan, K. Transport properties of 1,1,2,2-tetrafluoroethane (R134a). *Int. J. Thermophys.* **1993**, *14*, 951–988.

(12) Hammerschmidt, U. Thermal conductivity of a wide range of alternative refrigerants. Measured with an improved guarded hot-plate apparatus. *Int. J. Thermophys.* **1995**, *16*, 1203–1211.

(13) Tsvetkov, O. B.; Laptev, Y. A.; Asambaev, A. G. Experimental study and correlation of the thermal conductivity of 1,1,1,2-tetrafluoroethane (R134a) in the rarefied gas state. *Int. J. Refrig.* **1995**, *18*, 373–377.

(14) Gross, U.; Song, Y. W.; Hahne, E. Thermal conductivity of the new refrigerants R134a, R152a, and R123 measured by the transient hot-wire method. *Int. J. Thermophys.* **1992**, *14*, 957–983.

(15) Tanaka, Y.; Nakata, M.; Makita, T. Thermal Conductivity of Gaseous HFC-134a, HFC-143a, HCFC-141b, and HCFC-142b. *Int. J. Thermophys.* **1991**, *12*, 949–963.

(16) Yata, J.; Ueda, Y.; Hori, M. Equations for the Thermal Conductivity of R-32, R-125, R-134a, and R-143a. *Int. J. Thermophys.* **2005**, *26*, 1423–1435.

(17) Assael, M. J.; Leipertz, A.; MacPherson, E.; Nagasaka, Y.; Nieto de Castro, C. A.; Perkins, R. A.; Strom, K.; Vogel, E.; Wakeham, W. A. Transport property measurements on the IUPAC sample of 1,1,1,2-tetrafluoroethane (R134a). *Int. J. Thermophys.* **2000**, *21*, 1–22.

(18) Luettmer-Strathmann, J.; Sengers, J. V. The Thermal Conductivity of R134a in the Critical Region. *High Temp. High Press.* **1994**, *26*, 673–682.

(19) Hohenberg, P. C.; Halperin, B. I. Theory of dynamic critical phenomena. *Rev. Mod. Phys.* **1977**, *49*, 435–479.

(20) Hanley H. J. M.; Sengers J. V.; Ely J. F. On Estimating Thermal Conductivity Coefficients in the Critical Region of Gases. In *Thermal Conductivity 14*; Klemens, P. G., Chu, T. K., Eds.; Plenum Press: N.Y., 1976; pp 383−407.

(21) Garrabos, Y. Phenomenological Scale Factors for the Liquid-Vapor Critical Transition of Pure Fluids. *J. Phys. (Paris)* **1985**, *46*, 281–291.

(22) Le Neindre, B.; Garrabos, Y. Tufeu R. The critical thermal conductivity enhancement along the critical isochore. *Int. J. Thermophys.* **1991**, *12*, 307–321.

(23) McLinden, M. O.; Klein, S. A.; Lemmon, E. W.; Peskin, A. W. *NIST Standard Database 23, REFPROP Version 6.01*; Nat. Inst. Stand. Technol.: Boulder, CO, 1998.

(24) Garrabos, Y.; Palencia, F.; Lecoutre, C.; Erkey, C.; Le Neindre, B. Master singular behavior from correlation length measurements for seven one-component fluids near their gas-liquid critical point. *Phys. Rev. E* **2006**, *73*, 026125.

(25) Garrabos, Y.; Lecoutre, C.; Palencia, F.; Broseta, D.; Le Neindre, B. Master singular behaviour for the Sugden factor of one-component fluids near their gas-liquid critical point. *Phys. Rev. E* **2007**, *76*, 061109.

(26) Moldover, M. R.; Sengers, J. V.; Gammon, R. W.; Hocken, R. J. Gravity Effects in Fluids near the Gas-Liquid Critical Point. *Rev. Mod. Phys.* **1979**, *51*, 79–99.

(27) Sengers, J. V.; Levelt Sengers, J. M. H. Critical phenomena in classical fluids. *Progress in Liquid Physics*; C.A. Croxton: New York, 1978; Chapter 4, pp 103−174.

(28) Garrabos, Y.; Lecoutre, C.; Palencia, F.; Le Neindre, B.; Erkey, C. Master crossover functions for one-component fluids. *Phys. Rev. E* **2008**, *77*, 021116.

Received for review February 23, 2009. Accepted May 11, 2009.

JE900210H